Published in final edited form as:
Arterioscler Thromb Vasc Biol. 2012 November ; 32(11): 2702–2710. doi:10.1161/ATVBAHA.112.300115.

Decreased KRIT1 expression leads to increased vascular permeability and modifies inflammatory responses in vivo

Maripat Corr, M.D.[‡], **Irina Lerman**[*], **Julia M. Keubel**[*], **Lisa Ronacher**[‡], **Ravi Misra, Ph.D.**[†], **Frances Lund, Ph.D.**[†], **Ingrid H. Sarelius, Ph.D.**[*], and **Angela J. Glading, Ph.D.**[*,§]

[*]Department of Pharmacology and Physiology, University of Rochester, Rochester, NY

[†]Department of Medicine, Division of Allergy/Immunology and Rheumatology, University of Rochester, Rochester, NY

[‡]Department of Medicine, University of California, San Diego, La Jolla, CA

Abstract

Objective—The regulation of vascular permeability, leukocyte trafficking, and the integrity of endothelial cell-cell contacts are closely linked by a complex mechanism of inter-regulation. Here we investigate the role of KRIT1, an adherens junction accessory protein required for cell-cell junction stability, in the regulating these vascular functions.

Methods and Results—*Krit1*$^{+/-}$ mice exhibited an enhanced edematous response to the complex inflammatory stimuli found in the passive K/BxN model of inflammatory arthritis and the murine air pouch model, yet leukocyte infiltration was unchanged. Correspondingly, reduced KRIT1 expression increased baseline arteriole and venule permeability 2-fold over that of wildtype littermates, as measured by intravital microscopy of the intact cremaster muscle vascular network, but this increase was not accompanied by increased leukocyte extravasation or activation. Direct stimulation with tumor necrosis factor–α induced increased permeability in wildtype mice, but surprisingly, no increase over baseline levels was observed in *Krit1*$^{+/-}$ mice, despite extensive leukocyte activation. Finally, adoptive transfer of *Krit1*$^{+/-}$ bone marrow failed to increase permeability in wildtype mice. However, reduced expression of KRIT1 in the hematopoietic lineage dampened the differences observed in baseline permeability.

Conclusions—Taken together, our data indicate an integral role for KRIT1 in microvessel homeostasis and the vascular response to inflammation.

Keywords

permeability; vascular biology; arthritis; inflammation; CCM1

Vascular permeability is an important function of our cardiovascular system, controlling fluid balance and governing the movement of protein and cells into tissue. Permeability is cooperatively regulated by many inputs, including those from circulating blood cells, neighboring endothelial and smooth muscle cells, and the surrounding tissue. Central to our

[§]Corresponding author: Angela J. Glading Ph.D., University of Rochester, Department of Pharmacology and Physiology, 601 Elmwood Ave., Box 711, Rochester, NY 14642, Fax: (585) 273-2652, Phone: (585) 273-5750. angela_glading@urmc.rochester.edu.

The authors have no conflicts to disclose.

current understanding of vascular permeability is the regulation of endothelial cell-cell contacts, which contain the structural components, i.e. the cadherin-based adherens junctions and tight junctions, which form the functional barrier of the vessel wall. Much of what is currently understood about the regulation of endothelial cell-cell contacts, and by extension microvessel permeability, is derived from studies in which reversible increases in permeability are induced by inflammatory stimuli [1]. Importantly, many of the signals transduced by a variety of inflammatory signals functionally regulate endothelial permeability by altering the stability and localization of the adherens junction protein VE-cadherin [2, 3], suggesting that this may be the final step required for permeability changes, though other adherens and tight junction molecules may play a role. Based on findings in inflammation models, it is assumed that the endothelial cell-cell contact is also the site of permeability regulation under non-inflammatory, or homeostatic, conditions. However, direct manipulation of these contacts in vivo, for example by genetically deleting or mutating VE-cadherin or the junctional molecules p120 or β–catenin, leads to developmental vascular defects that prevent the study of microvessel permeability in situ [4-7]. Thus, our understanding of how changes in the stability of the endothelial junction complex affect microvessel permeability is hampered by a lack of appropriate animal models.

KRIT1, an 80kDa scaffolding protein, is a member of a multiprotein complex that promotes endothelial adherens junction stability *in vitro* [8]. In the human population, heterozygous loss-of-function mutations of KRIT1 cause cerebral cavernous malformation (CCM), a vascular malformation characterized by defective endothelial cell junctions and hemorrhage [9]. Though global or endothelial specific deletion of Krit1 is embryonic lethal during early vascular development (E9.5) [10], heterozygous mice ($Krit1^{+/-}$) are viable and model the genetic alteration found in human CCM patients. Our previous studies established a role for KRIT1 in endothelial cells in vitro, where the protein promotes the association of p120 and β–catenin with the cytoplasmic tail of VE-cadherin, thus stabilizing adherens junctions and promoting barrier function [11]. Even partial (~50-60%) loss of KRIT1 in vitro is sufficient to increase flux of small molecules across an endothelial monolayer [8], and reduces binding of β– and p120-catenin to the cytoplasmic tail of VE-cadherin [11]. In vivo studies using Krit1 heterozygous mice have demonstrated increased Evans Blue extravasation (Miles assay) in lung and brain tissues, particularly in response to lipopolysaccharide (LPS, [12]). While these findings point to an increase in protein and/or fluid flux across the vascular wall in the partial absence of Krit1, an important caveat to the Miles assay is that dye flux reflects the combined contribution of hydrostatic forces and vessel permeability. Thus the role of KRIT1 in the context of vascular permeability regulation – i.e. barrier function– in normal vessel physiology warrants further investigation in vivo.

The contribution of KRIT1 to barrier function in vitro suggests that alterations in Krit1 expression could modify physiological responses that require complex changes in vascular permeability by affecting the stability of endothelial cell-cell contacts. Herein we report that decreased KRIT1 expression results in a heightened response to inflammatory stimuli in mouse models of inflammatory arthritis and edema. This response correlates with increased baseline microvessel permeability to albumin in the intact vascular networks in situ. We further explore the relative contribution of Krit1 expression in endothelial and hematopoietic cell populations to the observed defects in barrier function, revealing an unexpected role for KRIT1 in permeability regulation by hematopoietic cells.

Methods

Mice

KRIT1 heterozygous (*Krit1*$^{+/-}$) mice were obtained from Dr. Dean Li (University of Utah). These mice are on a clean C57BL/6 background after having been backcrossed 10 generations to C57BL/6NCrl (Charles River Labs, stock #027). B6.SJL-*Ptprc*^{a} *Pepc*^{b}/BoyJ mice (CD45.1 B6) were obtained from Jackson Laboratory. KRN T cell receptor (TCR) transgenic mice were a gift from Drs. D. Mathis and C. Benoist (Harvard Medical School, Boston, MA and Institut de Génétique et de Biologie Moléculaire et Cellulaire, Strasbourg, France), and were maintained on a C57BL/6N background (K/B) [13]. Arthritic mice were obtained by crossing K/B with NOD/Lt (N) animals (K/BxN). Mice were bred and maintained under standard conditions in the University of California, San Diego (UCSD) animal facility (KRN, NOD/Lt, K/BxN and some *Krit1*$^{+/-}$) or the University of Rochester animal facility (*Krit1*$^{+/-}$ and CD45.1 B6), which are accredited by the American Association for Accreditation of Laboratory Animal Care. All protocols were approved by the respective institutional review board. All mice were used between 8 and 12 weeks of age; littermate controls were used in all experiments.

Statistics

Statistical analysis was performed using PRISM software (version 4.0, GraphPad Software Inc., La Jolla, CA). Significance was set at α=0.05.

Serum transfer and arthritis scoring

Arthritic adult K/BxN mice were bled and their sera were pooled. Age-matched male *Krit1*$^{+/-}$ or *Krit1*$^{+/+}$ littermates were injected with 50μl i.p. on Day 0 and Day 2 (n=9 mice/group) or 150 μl i.p. on Day 0 (n=20 mice/group). Clinical arthritis scores were evaluated using a scale of 0–4 for each paw (0, normal; 1, minimal erythema and mild swelling; 2, moderate erythema and mild swelling; 3, marked erythema and severe swelling, digits not yet involved; 4, maximal and swelling, digits involved) for a maximum score of 16. Ankle thickness in mm was measured with a caliper (Manostat, Switzerland). Change in ankle thickness was calculated as increase in size relative to baseline taken prior to serum administration. Statistical analysis was performed using 2-way ANOVA and Bonferroni post-hoc testing.

Miles Assay

Male *Krit1*$^{+/-}$ or *Krit1*$^{+/+}$ littermates (n=8 mice/group) were injected with either K/BxN serum or normal saline, 200μl i.p.: after 15 minutes mice 1mg/ml Evan's Blue dye (Sigma, St. Louis, MO) was injected via tail vein[14]. Fifteen minutes following dye injection the mice were bled into EDTA coated capillary tubes and serum collected by centrifugation. The mice were then perfused with PBS for 3 minutes to eliminate circulating dye. The wrists and ankles were harvested individually and extracted with formamide (Sigma). Supernatants were transferred to a 96 well flat bottom plate for absorbance measurement (600nm). Values were normalized to serum, and statistical analysis was performed using ANOVA and Tukey post-hoc testing.

Histology

Whole hind paws (n=8 mice/group) were fixed in 10% formalin, decalcified, trimmed and embedded. Sectioned tissue was stained with H&E and Safranin O (HistoTox, Boulder CO). Joints of arthritic mice were given scores of 0-4 for inflammation, according to the following criteria: 0 = normal; 1 = minimal infiltration of inflammatory cells in periarticular area; 2 = mild infiltration; 3 = moderate infiltration; and 4 = marked infiltration. Cartilage

depletion was identified by the presence of diminished Safranin O staining of the matrix and was scored on a scale of 0-4, where 0 = no cartilage destruction (full staining with Safranin O), 1 = localized cartilage erosions, 2 = more extended cartilage erosions, 3= severe cartilage erosions and 4 = depletion of entire cartilage. Histologic analyses were performed in a blinded manner.

Intravital Microscopy

Male wildtype (*Krit1*$^{+/+}$) or KRIT1 heterozygous null (*Krit1*$^{+/-}$) mice were anesthetized with sodium pentobarbital (65 mg/kg by i.p.) and maintained on supplemental anesthetic via a jugular catheter as needed. The cremaster muscle was prepared, superfused and visualized using established methods [15, 16]. Permeability to bovine serum albumin (BSA) was measured as described elsewhere [16]. The vascular wall P_s is calculated from the measured flux (J_s, mol/sec) of BSA into the tissue [17], with corrections for the source volume and surface area due to the confocal slice. In selected animals, the tissue was activated by intrascrotal injection of mouse recombinant tumor necrosis factor-α (TNF-⟨, 0.5μg in 0.25 ml saline, Sigma) or interleukin-1-β (IL-1β, 30ng in 0.25ml saline, Sigma) 3 hours before beginning the surgical preparation. Alternatively, 30μM histamine (Sigma) was added to the superfusate 5 min prior to image acquisition. On completion of the protocols, animals were euthanized by anesthetic overdose. For all permeability experiments, images were acquired from at least 9 vessel sites, which are the appropriate determinant for n in these experiments. Power analysis appropriate for ANOVA (F-test power) indicates that n=9, with a effect size of 0.2, and significance level of 0.05, results in a power level of 0.90. Data were analyzed using one-way ANOVA with Bonferroni post-hoc testing.

Cell culture and transfection

Human dermal microvascular endothelial cells were obtained from Lonza (Walkerville, PA), maintained in endothelial growth medium-2 (Lonza), and used prior to passage 6. Mouse dermal microvascular endothelial cells were obtained from Cell Biologics (Chicago, IL), maintained in mouse endothelial cell medium (Cell Biologics), supplemented with 10% fetal bovine serum, 10% *Krit1*$^{+/+}$ mouse serum, or 10% *Krit1*$^{+/-}$ mouse serum. Mouse serum was obtained by bleeding into EDTA coated capillary tubes followed by centrifugation. Cells were transfected with non-targeting negative control siRNA and anti-KRIT1 siRNA (Ambion/Invitrogen; ID#146530) as previously reported [8].

RNA isolation and semi-quantitative RT-PCR

RNA was isolated using the RNeasy Micro kit according to the manufacturer's instructions (Qiagen, Germantown, MD). Complementary DNA was obtained with Superscript III reverse transcriptase using random hexamers (Invitrogen, Grand Island, NY). Taqman assays for human ICAM-1 (Assay ID: Hs00164932_m1), human Krit-1 (Hs00184988_m1), human β-actin (401846) and human GAPDH (Hs99999905_m1) were purchased from Applied Biosystems (Invitrogen). VEGF primers are listed in supplemental methods. Amplifications were run in a 7000 Real-Time PCR system (Applied Biosystems/Invitrogen). Each value was calculated using the comparative Ct method [18] and normalized to internal controls. All samples were run in at least triplicate, and each experiment was performed from 3 separate cell/RNA preparations (n=3). Data were analyzed using 2-way ANOVA with Bonferroni post-hoc testing.

Adoptive bone marrow transfer

Bone marrow recipient adult male B6.SJL-*Ptprc*^{a} *Pepc*^{b}/BoyJ and *Krit1*$^{+/-}$ mice (8mice/group) were irradiated (475 Rads) twice 4 hours apart, using the Gammacell40 Cesium irradiator (Theratronics, Ottowa, ON). Immediately following the irradiations, mice were

anesthetized with isofluorane (Baxter International, Deerfield, IL) and injected i.v. with 1×10^6 bone marrow cells in 200 μl of HBSS (Mediatech, Manassas, VA). Mice were rested for 8 weeks to allow for complete immune system reconstitution. To evaluate the effectiveness of the bone marrow transplant, peripheral blood cells were isolated from the chimeric mice and analyzed by flow cytometry using antibodies specific for mouse CD45.1 (BD Biosciences, San Jose, CA), CD45.2 (eBioscience) and B220 (BD Biosciences). Data files containing live (propidium iodide negative) cells were collected on an Accuri C6 flow cytometer (BD Biosciences) and analyzed using FlowJo software (Tree Star, Ashland, OR).

Air pouch

The murine air pouch model was performed as described in [19]. Briefly, sequential subcutaneous injections of 5ml and 3ml sterile air were performed 72 hours apart on age- and sex- matched isoflurane anesthetized *Krit1*$^{+/+}$ or *Krit1*$^{+/-}$ mice (n=9/group). Seventy-two hours later, the mice were again anesthetized, and the air pouch was filled with 1.1ml sterile 1% carageenan dissolved in PBS (Sigma), or PBS alone. 24 hours later, the exudate was removed using an 18-gauge needle, and the volume and number of cells in the exudate quantified. Cell type distribution was quantified by visual counting of Giemsa stained cells. Statistical analysis was performed using ANOVA with Bonferroni post-hoc testing.

CBC

Complete blood counts and differential blood cell analysis were performed by the UCSD Animal Care Program Diagnostic Laboratory, n=3.

Leukocyte interactions

Bright-field images used to track leukocyte interactions with the vessel wall were acquired with a CCD camera (Dage-MTI CD72). Delivered leukocytes (cells translating in proximity to the vessel wall but not necessarily in continuous contact) were counted per 40 sec time interval. For each experimental group, at least 17 vessel sites were analyzed. Rolling leukocytes were defined as any leukocytes observed translating along the vessel wall continuously in contact with the endothelium for 1 sec or greater as defined in [15, 20]. Rolling leukocyte velocity was measured by tracking the distance rolled by individual cells for a period of time greater than 0.15 sec (at least 10 frames) within a 50μm length of vessel. All cells meeting our imaging criteria were analyzed from 17 vessel sites/group. Firmly adhered leukocytes (those remaining stationary for ≥ 30 sec) were counted in 10 vessel sites/group. Cell extravasation was measured as the number of cells in the tissue within 40μm of the vessel wall along a defined vessel length; for each condition, ≥ 9 vessel sites were analyzed. Data were analyzed using one-way ANOVA with Bonferroni post-hoc testing.

Supplemental Methods

TNF-α levels in air-pouch exudates were measured using the mouse TNF-a ELISA Ready-Set-Go assay from eBioscience (San Diego, CA). NFκB reporter assays were performed using the Dual-Glo luciferase assay system (Promega, Madison, WI) according to the manufacturer's instructions. Cell surface expression of 6 hematopoetic cell markers was measured by antibody labeling, followed by FACS analysis. Serum levels of inflammatory cytokines/chemokines were measured in duplicate using a multiplex bead assay (Eve Technologies, Calgary). Additional information is provided in Supplemental Materials available online.

Results

Effect of Krit1 haploinsufficiency on the development of inflammatory arthritis

We postulated that in *Krit1*$^{+/-}$ mice, the decrease in junction complex stability could affect their ability to maintain vascular barrier function in response to inflammatory stimuli. Therefore we assessed inflammatory responses in these mice using the K/BxN model of inflammatory arthritis. This is a well-characterized model of rheumatoid arthritis and is serum-transferable to normal recipients, allowing for the study of inflammatory arthritis in other mouse lines without the need for backcrossing [21]. This model is marked by a predominantly neutrophil infiltrate and edema, which resolve over time [22].

To measure the sensitivity of *Krit1*$^{+/-}$ mice to inflammatory stimuli, we performed two sequential injections of 50μl of K/BxN serum, which induced a sub-maximal inflammatory response as shown by the number of involved joints (Figure 1C). This dosing regimen was sufficient to induce swelling and arthritis in *Krit1*$^{+/-}$ mice, however this response was absent in wildtype animals (Figure 1A), indicating *Krit1*$^{+/-}$ mice are more sensitive to the induction of inflammation. A higher single dose of 150μl also induced a severe polyarthritis in both *Krit1*$^{+/-}$ and wildtype littermates (Figure 1B). At this dose, both groups developed arthritis to the same degree over the course of the experiment (Figure 1D). However, even at the higher serum dose, the *Krit1*$^{+/-}$ mice exhibited a significant increase in ankle thickness versus wildtype controls by 4 days post-serum injection, which continued until 7-days post injection at which time the inflammation began to resolve (Figure 1B). Both groups reached their maximum change in ankle size at Day 7, suggesting that the severity, and not the progression of the inflammation was affected.

To examine whether the increase in ankle thickness was due to an increase in microvascular leak in response to K/BxN serum, we injected Evans Blue dye 15 minutes prior to injection of serum, then quantified dye accumulation in the paws and feet (representative images shown in Supplemental Figure I) following formamide extraction. As expected, microvascular dye flux was increased in response to K/BxN serum in *Krit1*$^{+/-}$ animals compared to wildtype controls (Figure 2A). In addition, we examined the influx of inflammatory cells into the ankle joint of arthritic animals by immunohistochemistry. Ankle sections taken at the peak of cellular infiltration (Day 9) from a separate cohort of mice treated in an identical manner were stained with hematoxylin and eosin to assess leukocyte infiltration and bone erosion (i.e. inflammation) and with Safranin O to evaluate peptidoglycan loss and cartilage destruction. All sections were scored by an observer blinded to section identity using an established scale [23]. While a slight trend towards decreased inflammatory and erosion scores in *Krit1*$^{+/-}$ mice was observed, this was not statistically significant (Figure 2B). Representative images are shown in Figure 2C; un-injected tissue is shown for comparison. Arrowheads indicate areas of leukocyte infiltration; asterisks denote cartilage degradation. Thus inflammatory activation by K/BxN serum triggered a larger increase in protein flux across the vessel wall in *Krit1*$^{+/-}$ mice, but did not affect the accumulation of leukocytes in the inflamed joint.

Reduced KRIT1 expression increases baseline microvessel permeability

Our studies using the passive K/BxN arthritis model indicated that reduced expression of KRIT1 increases the flux of protein rich fluid into the tissue during inflammation, supporting our hypothesis that *Krit1*$^{+/-}$ mice exhibit defective fluid homeostasis. To examine whether these changes correlated with lower vascular barrier function in vivo, we directly measured the permeability (P_s) using intravital microscopy, under conditions in which changes in hydrostatic forces are minimal [16]. *Krit1*$^{+/-}$ arterioles exhibited a mean P_s of 1.646×10^{-6} cm/sec, significantly higher than that observed in wildtype littermates

(0.531×10^{-6} cm/sec, Table 1). As shown in Figure 3A, this difference is clearly due to both an overall upward shift in value, but also an increase in the variation of P_s values, including an increase in the proportion of highly leaky vessels. The effect of reduced KRIT1 expression in venules is less extreme (mean P_s of 1.383 vs. 0.664×10^{-6} cm/sec, Figure 3B, Table 1), but also clearly demonstrates an upward shift in permeability values. Thus reduced Krit1 expression is sufficient to reduce barrier function in vivo, confirming our earlier work in isolated cells. Notably, this increase was seen in the absence of any inflammatory stimulus, suggesting that KRIT1 haploinsufficiency predisposes these animals to edema formation.

Reduced KRIT1 expression blocks increased permeability in response to TNF–α, but not histamine

We then asked whether the increase in edema formation in the K/BxN model was the result of an increase in P_s in response to the inflammatory stimulus. This model relies on cytokine-dependent processes to trigger edema formation and leukocyte migration. Specifically, those mediated by increased expression of TNF–α and/or IL-1β [19, 24], common inflammatory signals released by leukocytes during inflammatory activation [25]. Therefore, we assessed permeability changes in response to TNF–α and IL-1β stimulation.

Injection of IL-1β 1-4 hours prior to imaging failed to induce significant changes in P_s in control or *Krit1*$^{+/-}$ animals, while triggering a massive leukocyte response in both strains (data not shown). However, injection of TNF–α 4 hours prior to imaging increased both arteriolar and venular P_s ~2-fold in wildtype littermates (Figure 3A and B), in agreement with previous studies [15] which established that this dose of TNF-α induces a maximum increase in permeability. Intriguingly, TNF–α stimulation was unable to increase P_s in *Krit1*$^{+/-}$ venules (Figure 3B), and surprisingly decreased P_s in *Krit1*$^{+/-}$ arterioles, though this difference was not statistically significant. We considered whether the lack of permeability increase in response to TNF–α was due to altered responses to TNF–α in *Krit1*$^{+/-}$ animals. TNF–α levels were similar between groups (Supplemental Figure IIA), as was the serum levels of other inflammatory cytokines or chemokines (Supplemental Figure IIB and IIC). Thus the difference in responsiveness is unlikely to be explained by altered TNF–α or cytokine expression.

Furthermore, reduced KRIT1 expression in endothelial cells does not appear to affect the activation of the nuclear factor kappa-light-chain-enhancer of activated B cells (NFκB) pathway by TNF–α, considered a major regulatory link between cytokine stimulation and permeability regulation. Krit1 mRNA expression decreased by >60% following anti-Krit1 siRNA transfection of human dermal microvascular endothelial cells (MVEC, Supplemental Figure IIIB) [8]. Knockdown of Krit1 did not affect NFκB-dependent luciferase expression in response to TNF–α treatment (Supplemental Figure IIIA), nor did it alter the NFκB-dependent induction of ICAM-1 mRNA by TNF–α [26](Figure 3C). To examine whether the endothelial response was affected by environmental factors, we also cultured siRNA-transfected mouse dermal microvascular endothelial cells (mMVEC) in media containing 10% *Krit1*$^{+/+}$ (WT) or *Krit1*$^{+/-}$ serum. We observed a decrease in TNF-α induced ICAM expression in both negative control and Krit1 siRNA-transfected cells in the presence of *Krit1*$^{+/-}$ serum, decreasing from an ~18-fold increase to an ~8-fold increase. However, the physiological relevance of this change is uncertain, given that an 8-fold increase in expression is still a significant up-regulation. Thus the absence of a TNF–α–induced increase in permeability in *Krit1*$^{+/-}$ mice is not likely due to an inability of KRIT1-deficient endothelium to respond to TNF–α stimulation. Finally, the lack of a permeability change in the *Krit1*$^{+/-}$ mice in response to TNF–α is not due to the maximal loss of barrier function, as treatment of cremaster muscle preps with histamine, and acute mediator of the inflammatory response, increased P_s in both *Krit1*$^{+/+}$ and *Krit1*$^{+/-}$ venules (Figure 3B).

Contribution of the Krit1$^{+/-}$ leukocyte population to microvessel permeability

We then examined the possibility that the role of KRIT1 in vascular permeability regulation may not be confined to its function in the endothelium. We had previously reported that KRIT1 protein is expressed in the hematopoietic lineage [11], and indeed appears to be expressed in most cell types. Furthermore, KRIT1 is an effector of the GTPase Rap1, a known modulator of leukocyte adhesion [27]. Given that the interplay between leukocyte and endothelial behavior is complex, it is difficult to predict the exact outcome of altered signaling between or within these two cell populations. Therefore, to examine the potential contribution of *Krit1*$^{+/-}$ leukocytes to edema formation and microvessel permeability, we generated reciprocal bone marrow chimeras.

We used congenic B6.SJL-*Ptprc*^{a} *Pepc*^{b}/BoyJ mice (referred to herein as CD45.1 B6) as the wildtype donor/recipient strain. These mice express the differential B cell antigen Ly5.1 (CD45.1), which allows differentiation between donor and recipient cell populations by fluorescence-activated cell sorting (FACS) analysis. *Krit1*$^{+/-}$ mice are on a C57BL/6N background, and express the *Ptprc*^{b} allele (CD45.2). Bone marrow cells isolated from either *Krit1*$^{+/-}$ or CD45.1 B6 donors were injected into irradiated *Krit1*$^{+/-}$ or CD45.1 B6 hosts. The four groups of mice, which included *Krit1*$^{+/-}$ bone marrow transferred into *Krit1*$^{+/-}$ recipients (*Krit1*$^{+/-}$ chimeras), CD45.1 B6 bone marrow into CD45.1 B6 recipients (CD45.1 B6 chimeras), *Krit1*$^{+/-}$ bone marrow into CD45.1 B6 recipients (*Krit1*$^{+/-\mathrm{BM}}$/B6$^{\mathrm{host}}$ chimeras) and CD45.1 B6 bone marrow into *Krit1*$^{+/-}$ recipients (B6$^{\mathrm{BM}}$/*Krit1*$^{+/-\mathrm{host}}$ chimeras) were allowed to reconstitute for 8 weeks, at which time peripheral blood cells were stained for CD45.1, CD45.2, and B220. In all four groups of mice, the percent reconstitution was greater than 95% (Supplemental Figure IV and Supplemental Table I).

We then measured P_s in the venules of recipient animals by intravital microscopy. Baseline permeability of the chimeric animals was increased compared to non-irradiated control animals (Figure 4A versus Figure 3A). However, similar to our previous observations using non-irradiated *Krit1*$^{+/-}$ and *Krit1*$^{+/+}$ mice, *Krit1*$^{+/-}$ chimeras exhibited a 3-fold increase in P_s compared to the CD45.1 B6 chimeras. The presence of *Krit1*$^{+/-}$ leukocytes in the *Krit1*$^{+/-\mathrm{BM}}$/B6$^{\mathrm{host}}$ chimeras slightly increased mean P_s over control levels (1.1 +/− 0.29 in *Krit1*$^{+/-\mathrm{BM}}$/B6$^{\mathrm{host}}$ chimeras versus 1.026 +/− 0.1433 in CD45.1 B6 chimeras), but did not rise to the levels observed in the *Krit1*$^{+/-}$ chimeras. Interestingly, mean P_s levels in the B6$^{\mathrm{BM}}$/*Krit1*$^{+/-\mathrm{host}}$ chimeras were not significantly different than the mean P_s levels in the control CD45.1 B6 chimeras, indicating that wild-type hematopoietic cells were sufficient to reverse the increased permeability observed in the *Krit1*$^{+/-}$ chimeras. Together, these data suggest, unexpectedly, that the observed increase in permeability in *Krit1*$^{+/-}$ mice is due to a requirement for Krit1 in both the hematopoietic and endothelial populations.

Reduced KRIT1 expression does not significantly promote leukocyte migration or adhesion

It is well established that leukocyte activation and adhesion plays an important role in the regulation of vascular permeability. Thus given the apparent contribution of hematopoietic cells to increased permeability in *Krit1*$^{+/-}$ mice, it appeared obvious to examine whether the increase in permeability was accompanied by a change in leukocyte behavior. Consequently, we utilized the air pouch inflammation model to study the effect of reduced expression of KRIT1 on leukocyte chemotaxis. We injected a previously created subcutaneous air space with either saline or carageenan, the latter of which induces fluid (exudate) accumulation and the infiltration of polymorphonuclear leukocytes (PMN) within 24 hours. There was no difference in leukocyte infiltration following carageenan treatment in *Krit1*$^{+/-}$ mice versus wildtype controls (Figure 4B), though we did observe a *Krit1*$^{+/-}$ dependent increase in exudate volume in carageenan treated mice (Figure 4C). Somewhat surprisingly, we

observed a small but significant increase in the number of cells found in the air pouch of saline-treated *Krit1*$^{+/-}$ mice (Figure 4B), concomitant with a significant increase in exudate volume (Figure 4C). The cells found in the exudate of carageenan treated mice and saline controls were primarily PMNs (>95%, data not shown), with a few monocytes present, suggesting some low level of inflammation is present even in saline controls. Thus reduced expression of Krit1 may increase leukocyte extravasation under sub-optimal inflammatory conditions, but has little to no effect on the leukocyte response to inflammatory stimuli.

As leukocyte migration is predicated on the adhesion of these cells to the vessel wall, we then directly examined leukocyte adhesion in microvessels, both in the absence of inflammation and following injection of TNF–α. Total white blood cell counts were equivalent and within the normal range in both strains (Figure 5A), and although the differential cell counts showed modest changes in some cell types, these were not significant and were not seen in a more detailed analysis of several hematopoetic markers (Supplemental Figure V). Subsequently, there was no difference between untreated *Krit1*$^{+/-}$ mice and wildtype littermate controls, in either the delivered (Figure 5B), or adhered (Figure 5C) leukocytes. Measurements were within the expected range for unstimulated vessels [20]. While *Krit1*$^{+/-}$ mice exhibited a slight increase in leukocyte transmigration, this was not statistically significant (Figure 5D). TNF–α induced a significant decrease in leukocyte rolling velocity (Figure 5E), and an increase in adhesion (Figure 5C) and the number of transmigrated cells (Figure 5D) in both groups of mice compared to untreated animals. The TNF–α response appeared as expected [15] in wildtype animals, and no significant increase in velocity, adhesion or extravasation in response to TNF–α was seen in *Krit1*$^{+/-}$ mice. Thus we conclude that under unstimulated conditions, *Krit1*$^{+/-}$ leukocytes do not exhibit increased activation, as measured by increased interaction with the vessel wall. Furthermore, these data suggest that the lack of permeability increase in response to TNF–α in *Krit1*$^{+/-}$ mice is not due to an inability of the leukocyte population to activate adhesion signaling in response to TNF–α stimulation.

Discussion

We have now clearly demonstrated that KRIT1 plays an integral role in microvessel homeostasis in vivo. Our data indicate that a reduction in KRIT1 expression leads to an increase in basal microvessel permeability in both arterioles and venules (Figures 3A and B), though the responses in these vessel types show subtle differences. We previously demonstrated, in wildtype animals, that flux occurs across the arteriolar wall, though to a lesser extent than in venules. *Krit1*$^{+/-}$ mice exhibit enhanced arteriolar permeability vs. venular permeability, suggesting that arteriolar endothelial cells may be more sensitive to loss of KRIT1 expression. Continued exploration of the KRIT1 function in specific vessel types is of particular interest, not the least because of the recent suggestion that CCM lesions are restricted to the venous network. Even so, loss of KRIT1 expression plainly has important implications for vascular homeostasis and edema formation during inflammation (Figure 1). Under homeostatic conditions, the increase in protein/fluid flux into the tissue in *Krit1*$^{+/-}$ mice appears to be compensated for by a concomitant increase in lymphatic drainage, as these mice do not exhibit edema when unchallenged. Following inflammatory stimuli, permeability may increase beyond the ability of the lymphatics to compensate, leading to severe swelling. This is seen most dramatically in the passive K/BxN model, in which reduced KRIT1 expression led to edema at a dose that did not induce a response in wildtype littermates (Figure 1A). However, we also demonstrated an enhanced response to inflammation in the air pouch synovitis model (Figure 4B and C) and following direct stimulation of a microvascular network in vivo (histamine, Figure 3D). The consequence of this higher basal permeability and sensitivity to inflammation in regards to the development of CCM are unclear. However, it is possible that alterations in the inflammatory response

could play a role in lesion development or severity. It has been suggested that the presence of inflammatory cells in CCM lesions is associated with risk of hemorrhage and significant symptomatic disease [28]. Thus inflammation could increase the relative risk of hemorrhage from the lesion, or the persistence of post-bleed symptoms. Current clinical practices make it difficult to assess this premise in the human population, but new mouse models of CCM will enable us to test this hypothesis in future studies.

Our initial hypothesis predicts that the mechanism that underlies the higher baseline permeability and increase in edema formation is likely downstream of the destabilizing effect of reduced KRIT1 expression on endothelial cell-cell junctions. This hypothesis was based in part on the assumption that the essential physiological functions of KRIT1 are confined to the endothelial compartment. Despite the fact that CCM patients exhibit a germline defect in Krit1 expression in all cell types, CCM is considered an endothelial disease, as mouse models indicate that loss of CCM proteins in endothelial cells is sufficient to generate lesion formation [29]. Therefore, we were very surprised to find that the increase in baseline permeability observed in *Krit1*$^{+/-}$ animals was completely blocked when the *Krit1*$^{+/-}$ mice were reconstituted with wildtype bone marrow (Figure 4A). This result contrasts with our findings in vitro, which indicated that reduced KRIT1 expression was sufficient to increase endothelial leak in the absence of immune cells [8]. Such differences highlight the need for in vivo studies, in which complex cellular interactions are present that may significantly affect the measured physiological responses.

Nonetheless, our findings suggest that *Krit1*$^{+/-}$ hematopoietic cells contribute to the enhanced permeability in *Krit1*$^{+/-}$ mice, a novel finding that opens many new channels of research. Cellular interactions between the vascular endothelial wall and leukocytes have a well-documented ability to modify vascular permeability, thus we closely examined this interaction in vivo. The interaction between leukocytes and the vessel wall occurs to a similar extent in unstimulated *Krit1*$^{+/-}$ mice compared to wildtype controls (Figure 5), under conditions in which the permeability change is evident (Figure 3A). Furthermore, adoptive transfer of *Krit1*$^{+/-}$ hematopoietic cells failed to increase permeability in wildtype animals (Figure 4A), and KRIT1 haploinsufficiency enhanced fluid extravasation during inflammation in both the K/BxN and air pouch models without significantly affecting leukocyte extravasation (Figures 1 and 4). While we did observe increased leukocyte extravasation in unstimulated *Krit1*$^{+/-}$ mice (Figure 4B), this likely reflects an increased likelihood for extravasation due to a decrease in barrier function, and the magnitude of this increase suggests this is unlikely to have physiological implications. It is perhaps more noteworthy that we now can show that full KRIT1 expression is not required for effective leukocyte adhesion, implying that Krit1 is unlikely to be a relevant Rap1 effector in this cell type. Despite these significant findings, future studies will be required to determine what hematopoietic cell compartment is responsible for the enhanced permeability response in *Krit1*$^{+/-}$ mice.

It is now apparent that the contribution of reduced KRIT1 expression in the hematopoietic compartment to vascular permeability is independent of leukocyte activation and adhesion, (Figure 5), and not due to global differences in cytokine or chemokine expression (Supplemental Figure IIB and IIC). Leukocytes can produce many permeability-inducing factors such as reactive oxygen species, and vascular endothelial growth factor (VEGF), commonly as part of the leukocyte activation process. Intriguingly, it was recently shown that reduced KRIT1 expression in endothelial cells is linked to increased reactive oxygen species signaling [30]. Furthermore, we previously published that reduced KRIT1 expression increases expression of VEGF in endothelial cells through activation of the canonical β-catenin pathway [11]. Indeed, we observed higher levels of serum VEGF in *Krit1*$^{+/-}$ mice as well as increased VEGF mRNA in isolated *Krit1*$^{+/-}$ bone marrow cells (Supplemental

Figure IIB and VI). Thus it is possible that changes in VEGF, reactive oxygen species, or other permeability inducing factors drive the increase in basal vascular permeability seen in *Krit1*$^{+/-}$ mice, a question we are actively pursuing in ongoing studies.

These data now bring into question the mechanism of KRIT1's biological effects. It appears clear that the overall physiological effect of KRIT1 haploinsufficiency is unlikely to be confined to its functions in the endothelial cell. Furthermore, we recently demonstrated that the Krit1 deficiency-induced decrease in cell contact stability leads to an increase in β–catenin dependent transcriptional activity in vitro and in vivo [11]. Thus the effects of KRIT1 deficiency in vivo, including the ability of the endothelium to respond to normal inflammatory stimuli, may extend beyond the stability of the cell-cell contact. This idea is supported by the inability of *Krit1*$^{+/-}$ mice to increase permeability in response to TNF–α treatment, yet these animals were able to respond to other permeability inducing factors—including histamine (Figures 3A and B), VEGF[31], and LPS [12]. This suggests that reduced KRIT1 expression does not merely reduce barrier function in vivo, but may actively modify signaling responses to inflammatory mediators.

In summary, our observations point to an important role for KRIT1 in maintaining normal microvessel homeostasis in vivo. Significantly, the requirement for reduced KRIT1 expression in the hematopoietic cell population for increased permeability may have implications for the pathophysiology of CCM. However, these studies also point to a role for KRIT1 in the regulation of barrier permeability in response to inflammation, and in particular the outcome of individual cytokine and chemokine signaling. Further dissecting these mechanisms will allow for a more detailed understanding of the regulation of microvessel permeability in response to these factors, and may provide important insights into the centrality of endothelial cell-cell contact in vascular permeability, including the relative contribution of the actions of the inflammatory stimuli directly on the structural barrier (i.e. endothelial-dependent effects) versus effects downstream of leukocyte activation and adhesion.

Supplementary Material

Refer to Web version on PubMed Central for supplementary material.

Acknowledgments

We thank Dr. Mark H. Ginsberg for critical review of the manuscript and valuable comments.

This work was supported by grants from the NIH HL18208 and HL75186 to I. Sarelius, NIH AI063399 to F. Lund, NIH F32AI080104 to R. Misra, Arthritis Foundation to M. Corr, and the American Heart Association to A. Glading (0930071N).

Non-standard Abbreviations and Acronyms

CCM	cerebral cavernous malformation
Krit1	Krev interaction-trapped 1
TNF–α	tumor necrosis factor-alpha
BSA	bovine serum albumin
MVEC	dermal microvascular endothelial cells

References

1. Lee WL, Liles WC. Endothelial activation, dysfunction and permeability during severe infections. Curr Opin Hematol. 2011; 18:191–196. [PubMed: 21423012]
2. London NR, Smith MC, Li DY. Emerging mechanisms of vascular stabilization. J Thromb Haemost. 2009; 7(Suppl 1):57–60. [PubMed: 19630769]
3. Dejana E, Tournier-Lasserve E, Weinstein BM. The control of vascular integrity by endothelial cell junctions: Molecular basis and pathological implications. Dev Cell. 2009; 16:209–221. [PubMed: 19217423]
4. Cattelino A, Liebner S, Gallini R, Zanetti A, Balconi G, Corsi A, Bianco P, Wolburg H, Moore R, Oreda B, Kemler R, Dejana E. The conditional inactivation of the beta-catenin gene in endothelial cells causes a defective vascular pattern and increased vascular fragility. J Cell Biol. 2003; 162:1111–1122. [PubMed: 12975353]
5. Oas RG, Xiao K, Summers S, Wittich KB, Chiasson CM, Martin WD, Grossniklaus HE, Vincent PA, Reynolds AB, Kowalczyk AP. P120-catenin is required for mouse vascular development. Circ Res. 2010; 106:941–951. [PubMed: 20110533]
6. Wallez Y, Huber P. Endothelial adherens and tight junctions in vascular homeostasis, inflammation and angiogenesis. Biochim Biophys Acta. 2008; 1778:794–809. [PubMed: 17961505]
7. Vittet D, Buchou T, Schweitzer A, Dejana E, Huber P. Targeted null-mutation in the vascular endothelial-cadherin gene impairs the organization of vascular-like structures in embryoid bodies. Proc Natl Acad Sci U S A. 1997; 94:6273–6278. [PubMed: 9177207]
8. Glading A, Han J, Stockton RA, Ginsberg MH. Krit-1/ccm1 is a rap1 effector that regulates endothelial cell cell junctions. J Cell Biol. 2007; 179:247–254. [PubMed: 17954608]
9. Labauge P, Denier C, Bergametti F, Tournier-Lasserve E. Genetics of cavernous angiomas. Lancet Neurol. 2007; 6:237–244. [PubMed: 17303530]
10. Whitehead K, Plummer N, Adams J, Marchuk D, Li D. Ccm1 is required for arterial morphogenesis: Implications for the etiology of human cavernous malformations. Development. 2004; 131:1437–1448. [PubMed: 14993192]
11. Glading AJ, Ginsberg MH. Rap1 and its effector krit1/ccm1 regulate beta-catenin signaling. Dis Model Mech. 2010; 3:73–83. [PubMed: 20007487]
12. Stockton RA, Shenkar R, Awad IA, Ginsberg MH. Cerebral cavernous malformations proteins inhibit rho kinase to stabilize vascular integrity. J Exp Med. 2010; 207:881–896. [PubMed: 20308363]
13. Kouskoff V, Korganow AS, Duchatelle V, Degott C, Benoist C, Mathis D. Organ-specific disease provoked by systemic autoimmunity. Cell. 1996; 87:811–822. [PubMed: 8945509]
14. Miles AA, Miles EM. Vascular reactions to histamine, histamine-liberator and leukotaxine in the skin of guinea-pigs. J Physiol. 1952; 118:228–257. [PubMed: 13000707]
15. Sumagin R, Kuebel JM, Sarelius IH. Leukocyte rolling and adhesion both contribute to regulation of microvascular permeability to albumin via ligation of icam-1. Am J Physiol Cell Physiol. 2011; 301:C804–813. [PubMed: 21653902]
16. Sarelius IH, Kuebel JM, Wang J, Huxley VH. Macromolecule permeability of in situ and excised rodent skeletal muscle arterioles and venules. Am J Physiol Heart Circ Physiol. 2006; 290:H474–480. [PubMed: 16126813]
17. Huxley VH, Curry FE, Adamson RH. Quantitative fluorescence microscopy on single capillaries: Alpha-lactalbumin transport. Am J Physiol. 1987; 252:H188–197. [PubMed: 3492924]
18. Livak KJ, Schmittgen TD. Analysis of relative gene expression data using real-time quantitative pcr and the 2(-delta delta c(t)) method. Methods. 2001; 25:402–408. [PubMed: 11846609]
19. Romano M, Faggioni R, Sironi M, Sacco S, Echtenacher B, Di Santo E, Salmona M, Ghezzi P. Carrageenan-induced acute inflammation in the mouse air pouch synovial model. Role of tumour necrosis factor. Mediators Inflamm. 1997; 6:32–38.
20. Sumagin R, Sarelius IH. Tnf-alpha activation of arterioles and venules alters distribution and levels of icam-1 and affects leukocyte-endothelial cell interactions. Am J Physiol Heart Circ Physiol. 2006; 291:H2116–2125. [PubMed: 16766643]

21. Kouskoff V, Korganow AS, Duchatelle V, Degott C, Benoist C, Mathis D. A new mouse model of rheumatoid arthritis: Organ-specific disease provoked by systemic autoimmunity. Ryumachi. 1997; 37:147. [PubMed: 9136609]
22. Wipke BT, Allen PM. Essential role of neutrophils in the initiation and progression of a murine model of rheumatoid arthritis. J Immunol. 2001; 167:1601–1608. [PubMed: 11466382]
23. Choe JY, Crain B, Wu SR, Corr M. Interleukin 1 receptor dependence of serum transferred arthritis can be circumvented by toll-like receptor 4 signaling. J Exp Med. 2003; 197:537–542. [PubMed: 12591910]
24. Kyburz D, Corr M. The krn mouse model of inflammatory arthritis. Springer Semin Immunopathol. 2003; 25:79–90. [PubMed: 12904893]
25. Madge LA, Pober JS. Tnf signaling in vascular endothelial cells. Exp Mol Pathol. 2001; 70:317–325. [PubMed: 11418010]
26. Ledebur HC, Parks TP. Transcriptional regulation of the intercellular adhesion molecule-1 gene by inflammatory cytokines in human endothelial cells. Essential roles of a variant nf-kappa b site and p65 homodimers. J Biol Chem. 1995; 270:933–943. [PubMed: 7822333]
27. Bos J. Linking rap to cell adhesion. Curr Opin Cell Biol. 2005; 17:123–128. [PubMed: 15780587]
28. Shi C, Shenkar R, Du H, Duckworth E, Raja H, Batjer HH, Awad IA. Immune response in human cerebral cavernous malformations. Stroke. 2009; 40:1659–1665. [PubMed: 19286587]
29. Chan AC, Drakos SG, Ruiz OE, Smith AC, Gibson CC, Ling J, Passi SF, Stratman AN, Sacharidou A, Revelo MP, Grossmann AH, Diakos NA, Davis GE, Metzstein MM, Whitehead KJ, Li DY. Mutations in 2 distinct genetic pathways result in cerebral cavernous malformations in mice. J Clin Invest. 2011; 121:1871–1881. [PubMed: 21490399]
30. Goitre L, Balzac F, Degani S, Degan P, Marchi S, Pinton P, Retta SF. Krit1 regulates the homeostasis of intracellular reactive oxygen species. PLoS One. 2010; 5:e11786. [PubMed: 20668652]
31. Whitehead KJ, Chan AC, Navankasattusas S, Koh W, London NR, Ling J, Mayo AH, Drakos SG, Marchuk DA, Davis GE, Li DY. The cerebral cavernous malformation signaling pathway promotes vascular integrity via rho gtpases. Nat Med. 2009

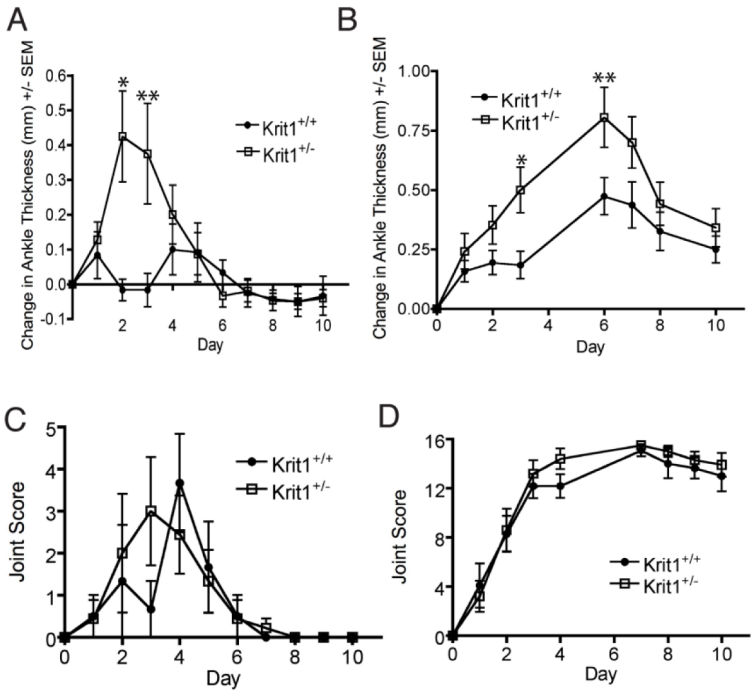

Figure 1. Reduced Krit1 expression enhances edema formation

A & C) Response to two 50μl doses of K/BxN serum. Change in ankle thickness is given relative to Day 0, *p<0.001, **p<0.01 vs. wildtype. Joint scoring, maximum score=16. B & D) Response to single 150μl dose of K/BxN serum, Change in ankle thickness, *p<0.05, **p<0.01 vs. wildtype. Joint scoring, maximum score=16.

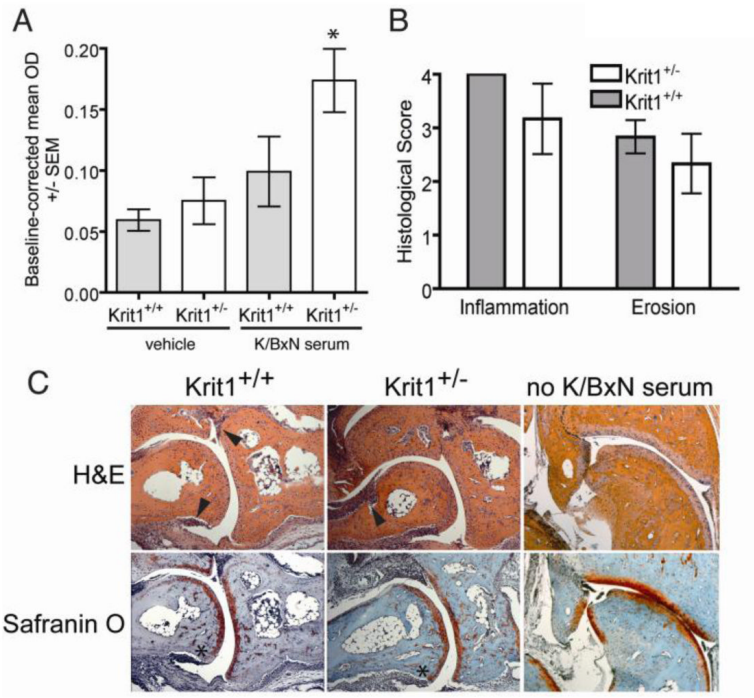

Figure 2. Reduced Krit1 expression increases edema formation but not leukocyte infiltration in response to K/BxN serum

A) OD values from formamide extracted paws and feet normalized to serum dye OD, *p<0.05 vs. wildtype + K/BxN serum. B) Mean histological scoring of mice at Day 9 following administration of 150μl of K/BxN serum, +/− SD. C) Representative brightfield images (50x magnification) of inflammation in the talo-navicular joints of animals used for histological scoring. H&E (hematoxylin and eosin) shows general tissue morphology and presence of leukocyte infiltration (arrowheads); Safranin O staining demonstrates local erosion of bone (light blue/purple) and cartilage (red) (asterisks).

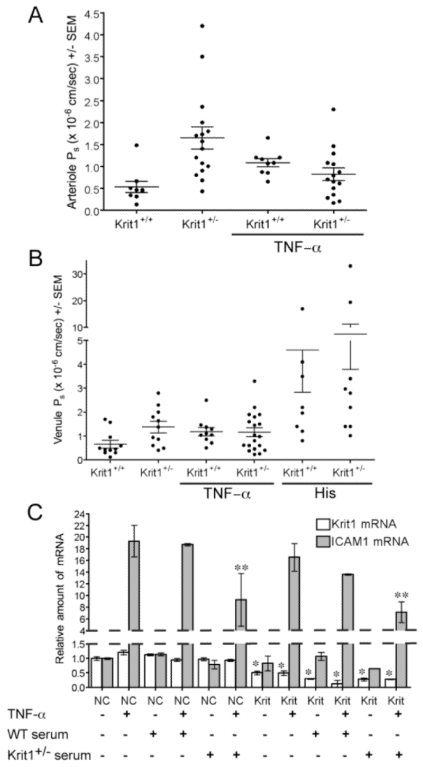

Figure 3. Reduced Krit1 expression directly alters microvessel permeability

A) Permeability of albumin in arterioles of *Krit1*$^{+/-}$ and *Krit1*$^{+/+}$ mice. Data shown is mean P_s +/− SEM, Overall p<0.0001 by ANOVA. B) Permeability of albumin in venules of *Krit1*$^{+/-}$ and *Krit1*$^{+/+}$ mice. Overall p<0.001 by ANOVA. C) Relative ICAM-1 and Krit1 mRNA expression in siRNA-transfected mouse MVEC treated with either TNF–α, or serum isolated from *Krit1*$^{+/+}$ (WT) or *Krit1*$^{+/-}$ mice, or both. NC- negative control siRNA transfected cells, Krit1- anti-Krit1 siRNA transfected cells, n=3.

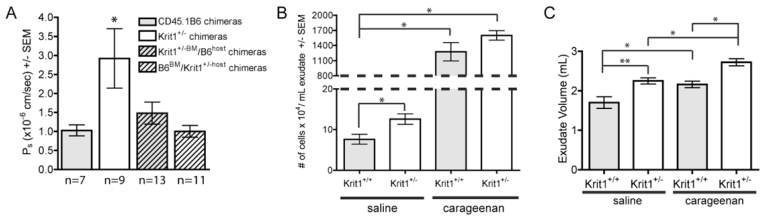

Figure 4. Reduced Krit1 expression in bone marrow derived cells is required for increased permeability; reduced Krit1 expression increases fluid extravasation in the murine air pouch model

A) Permeability of albumin in cremaster microvessels following adoptive transfer, * $p<0.01$ vs. CD45.1 B6 chimera. Number of vessels analyzed is indicated below columns. B) Number of cells recovered per milliliter exudate, *$p<0.01$. C) Recovered exudate volumes from saline and carageenan treated mice, *$p<0.05$, **$p<0.001$.

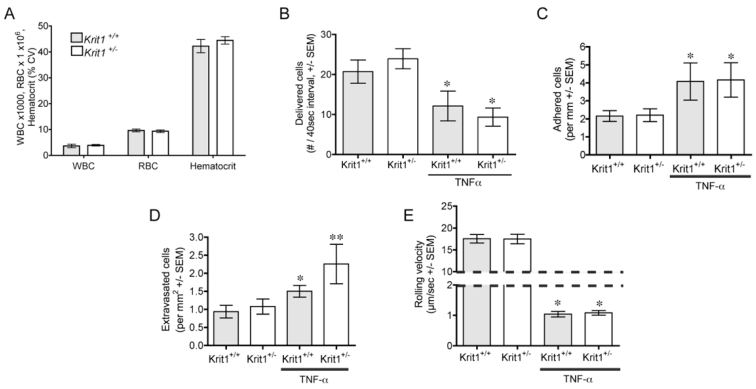

Figure 5. Reduced Krit1 expression does not affect leukocyte adhesion

A) Total cell counts from peripheral blood; WBC, white blood cells, RBC, red blood cells, +/− SEM. B) Delivered flux -visible fraction of leukocytes near the wall/40 sec- in unstimulated and TNF–α treated mice, *p<0.01 vs. untreated. C) Number of adhered leukocytes per mm vessel wall, *p<0.05 vs. untreated. D) Number of leukocytes within 40μm of the vessel wall, per mm^2, *p<0.05 vs. untreated *Krit1*$^{+/+}$, **p<0.05 vs. untreated *Krit1*$^{+/-}$. E) Rolling velocity of wall-associated leukocytes, *p<0.001 vs. untreated.

Table 1

Mean P_s values in microvessels of wildtype and *Kritl*$^{+/-}$ mice

Genotype	Microvessel type	Treatment	Mean P_s ($\times 10^{-6}$ cm/sec) +/− SEM	p value*	n=
Krit1 $^{+/-}$	*Arterioles*	none	1.646 +/− 0.25	<0.01	16
	Venules	none	1.383 +/− 0.24	<0.01	11
	Arterioles	TNF-α	0.820 +/− 0.15	n.s†	15
	Venules	TNF-α	1.158 +/− 0.19	n.s†	19
	Venules	His	7.510 +/− 1.72	<0.01	9
Krit1 $^{+/+}$	*Arterioles*	none	0.531 +/− 0.13	-	9
	Venules	none	0.664 +/− 0.16	-	11
	Arterioles	TNF-α	1.189+/− 0.09	<0.05	9
	Venules	TNF-α	1.189 +/− 0.17	<0.05	10
	Venules	His	4.607 +/− 1.77	<0.001	9

*p values are calculated versus wildtype for unstimulated vessels, and versus unstimulated vessels of same genotype for TNF-α and histamine treated animals.

†n.s.-not significant.

Arterioscler Thromb Vasc Biol. Author manuscript; available in PMC 2013 November 01.